

# DeepTopPush: Simple and Scalable Method for Accuracy at the Top

Lukáš Adam<sup>\*1,2</sup>, V. Mácha<sup>2</sup> and V. Šmídl<sup>2</sup>

<sup>1</sup>Southern University of Science and Technology, 1088 Xueyuan Avenue, Shenzhen 518055, China

<sup>2</sup>Institute of Information Theory and Automation, The Czech Academy of Sciences, Pod Vodárenskou věží 4, 18208, Prague, Czech Republic

June 19, 2020

## Abstract

Accuracy at the top is a special class of binary classification problems where the performance is evaluated only on a small number of relevant (top) samples. Applications include information retrieval systems or processes with manual (expensive) postprocessing. This leads to the minimization of irrelevant samples above a threshold. We consider classifiers in the form of an arbitrary (deep) network and propose a new method DeepTopPush for minimizing the top loss function. Since the threshold depends on all samples, the problem is non-decomposable. We modify the stochastic gradient descent to handle the non-decomposability in an end-to-end training manner and propose a way to estimate the threshold only from values on the current minibatch. We demonstrate the good performance of DeepTopPush on visual recognition datasets and on a real-world application of selecting a small number of molecules for further drug testing.

## 1 Introduction

Binary classifiers compute a score for each sample and then compare it with a given threshold to predict whether the sample belongs to the positive or negative class. This score is often interpreted as the probability that the sample is of the positive class and the threshold is usually 0.5. Such a task attempts to correctly classify all samples. However, in many applications, it is desirable to correctly classify only a small subset of samples with the highest scores. This arises in information retrieval systems where the user is interested only in a few queries or in situations where the samples undergo expensive further processing and only a small number of samples may be manually evaluated.

This task considers only scores which lie above or below a certain threshold. Due to this reason, the problem was named *Accuracy at the Top* in [6]. Since this threshold is no longer fixed, as in the case of 0.5, but depends on all samples, the objective cannot be expressed in an additive way (the objective is non-decomposable). As a result, stochastic gradient descent provides a biased gradient estimate and it is no longer directly applicable. We denote the pipeline of accuracy at the top in Figure 1.

There is a close connection between the accuracy at the top and ranking problems. A special case of the latter attempts to rank positive samples above negative samples. Several approaches, such as RankBoost [10], Infinite Push [3] or  $p$ -norm push [19] employ a positive-negative pairwise comparison of scores, which can handle only small datasets. TopPush [14] converts the pairwise

---

<sup>\*</sup>3@ieee.org

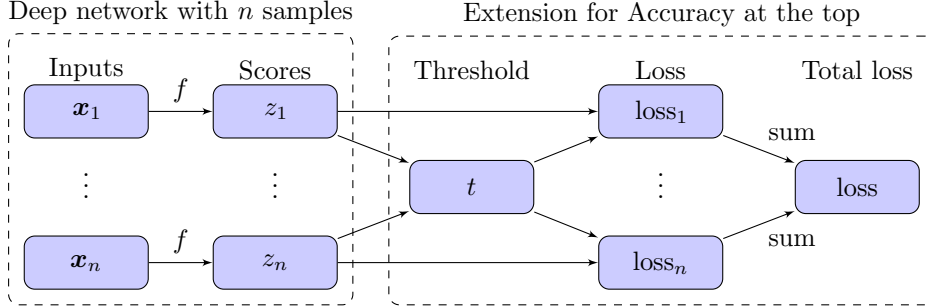


Figure 1: The pipeline of Accuracy at the top which also serves as a basis for *DeepTopPush*. For each input  $x_i$  an arbitrary network  $f$  computes its score  $z_i$ . The threshold  $t$  is a combination of all scores. For each sample, its loss is based on its distance from the threshold. The total loss sums these losses.

sum into a single sum and minimizes the false-negatives below a threshold given by the maximum score corresponding to negative samples. Thus, it converts ranking into the accuracy at the top problems.

Many approaches for handling the non-decomposability of the objective exist [4, 20]. We focus on two classes. Both of them use a classification network to compute the scores but differ in their representation of the threshold. The first class considers the threshold as a simple constraint. Since it employs theoretical reformulations, it usually restricts to convexity and linear classifiers. The second class uses heuristic approximations for the threshold computation.

In the first class, Acc@Top [6] argues that the threshold equals to one of the scores. They fix the index of a sample and solve as many optimization problems as there are samples. This makes the problem infeasible for large datasets. [7, 2, 16] follow a similar approach: they write the threshold as a constraint and replace both the objective and the constraint via surrogates. [7] uses Lagrange multipliers to obtain a minimax problem, [2] implicitly removes the threshold as an optimization variable and uses the chain rule to compute the derivatives while [16] solves an SVM-like dual formulation with kernels. [11] uses the same formulation but applies surrogates only to the objective and recomputes the threshold after each gradient step. In the second class, SoDeep [8] uses the fact that the threshold may be easily computed from sorted scores. They replace the right-hand side of Figure 1 by another network which approximates the sorting operator. The second network can be trained on artificial data, it is sensitive to the number of samples and the distribution of the artificial samples. AP-Perf [9] considers a general metric and hedges against the worst-case perturbation of scores. The authors argue that the problem is bilinear in scores and use duality arguments. However, the bilinearity is lost when optimizing with respect to the weights of the original network.

Our method *DeepTopPush* is simple but powerful. We consider accuracy at the top exactly as depicted in Figure 1. It has benefits of both classes mentioned earlier: the simplicity of the first and the possibility to use general networks of the second class. Due to non-decomposability, we need to propose a way of computing derivatives and incorporating the stochastic gradient descent. For the former, we combine several of the previously mentioned ideas. Since the threshold always equals to one of the scores [6], the threshold computation has a simple local formula. As the gradient is a local object, we implicitly remove some variables [2] and apply the chain rule (backpropagation) to compute the derivatives in an end-to-end manner. For the latter, we need to approximate the threshold, which is computed from all scores, based only on a minibatch. We follow the idea of [1] and stabilize the threshold by considering delayed values of the scores. The main contributions of the paper are as follows:

- We propose *DeepTopPush* which is a simple and scalable method for optimizing accuracy at the top. We propose a modified gradient descent algorithm for the non-decomposable loss.
- We show that *DeepTopPush* implies only a slight increase in the computational time, yet it

achieves better performance than prior art methods with a much higher computational cost.

- We show that the same theoretical analysis for *DeepTopPush* can be applied to a much larger class of optimization problems, containing e.g. maximizing precision at recall.

The paper is organized as follows: In Section 2 we introduce a general formulation of accuracy at the top and show which models from the literature fall into this setting. In Section 3 we propose *DeepTopPush*. We compute the derivatives and modify the stochastic gradient descent to handle the non-decomposable objective function. In Section 4 we show the good performance of *DeepTopPush* on multiple images recognition datasets and a real-world medical application. To promote reproducibility, all our codes are available online.<sup>1</sup>

## 2 Accuracy at the top

In this section, we show how to extend a deep network to handle the accuracy at the top in an end-to-end manner. A standard deep network takes inputs  $\mathbf{x}_i$ , transforms them into scores  $z_i$  and computes the total loss based on these scores and labels. The loss function of the accuracy at the top is based only on scores above (or below) a certain threshold, recall Figure 1. Its left-hand side contains any classifier  $f$  and computes the scores  $z_i$  while the right-hand side is the extension for maximizing accuracy at the top. Based on all scores, it computes the threshold  $t$ , the loss for each sample and the total loss. Since this threshold is a function of all scores, the problem is non-decomposable.

Writing this more formally, the optimization problem consists of minimizing the weighted sum of false-positives and false-negatives

$$\begin{aligned} & \underset{\mathbf{w}}{\text{minimize}} \quad \lambda_1 \text{fp}(\mathbf{z}, t) + \lambda_2 \text{fn}(\mathbf{z}, t) \\ & \text{subject to} \quad z_i = f(\mathbf{w}; \mathbf{x}_i), \\ & \quad t \text{ is a function of } \{z_i\}. \end{aligned} \tag{1}$$

Here,  $\mathbf{w}$  are the weights of the network and false-positives, false-negatives and true-positives are defined as follows

$$\text{fp}(\mathbf{z}, t) = \sum_{i \in I^-} \mathbb{1}_{z_i \geq t}, \quad \text{fn}(\mathbf{z}, t) = \sum_{i \in I^+} \mathbb{1}_{z_i < t}, \quad \text{tp}(\mathbf{z}, t) = \sum_{i \in I^+} \mathbb{1}_{z_i \geq t}, \tag{2}$$

where  $I^+$  is the set of positive labels,  $I^-$  is the set of negative labels and  $\mathbb{1}$  is the characteristic (0/1) function counting how many times the argument is satisfied.

We will show how the well-known problem of maximizing precision at a given level of recall

$$\begin{aligned} & \underset{\mathbf{w}}{\text{maximize}} \quad \text{Precision} \\ & \text{subject to} \quad \text{Recall} = \alpha \end{aligned} \tag{3}$$

falls into formulation (1). Since the constraint  $\text{Recall} = \alpha$  is equivalent to  $\text{tp}(\mathbf{z}, t) = n^+ \alpha$ , precision equals to

$$\text{Precision} = \frac{\text{tp}(\mathbf{z}, t)}{\text{tp}(\mathbf{z}, t) + \text{fp}(\mathbf{z}, t)} = \frac{n^+ \alpha}{n^+ \alpha + \text{fp}(\mathbf{z}, t)}.$$

Then maximizing precision is equivalent to minimizing false-negatives. Moreover,  $\text{Recall} = \alpha$  states that  $n^+ \alpha$  components of  $\mathbf{z}^+$  are above the threshold  $t$ . This can be restated by stating that  $t$  equals to the  $\lceil n^+ \alpha \rceil$ -largest component of  $\mathbf{z}^+$  equals to  $t$ . This yields the following problem

$$\begin{aligned} & \underset{\mathbf{w}}{\text{minimize}} \quad \text{fp}(\mathbf{z}, t) \\ & \text{subject to} \quad z_i = f(\mathbf{w}; \mathbf{x}_i), \\ & \quad t = z_{[i^*]}^+, \quad i^* = \lceil n^+ \alpha \rceil. \end{aligned} \tag{4}$$

---

<sup>1</sup><https://github.com/VaclavMacha/AccuracyAtTop.jl/tree/NeurIPS-v1>

Here, we employed the notation that  $z_{[1]} \geq \dots \geq z_{[n]}$  is the *non-increasing* sorted version of scores  $\mathbf{z} = (z_1, \dots, z_n)$ . Whenever (3) has a solution, this solution is recovered by solving (4). If (3) does not have a solution (which may happen if there are multiple scores  $z_i$  with the same value), then (4) provides its feasible approximation. Obviously, Prec@Rec problem (4) falls into setting (1).

We summarize additional problems which belong to the framework (1) in Table 1. For the definition of the problems and the derivations, we refer to Appendix A.

Table 1: Summary of problems which fall into setting (1). Weights  $\lambda_1$  and  $\lambda_2$  determine the objective, the threshold  $t$  may be computed from all/positive/negative scores and the index  $i^*$  defined via  $t = z_{[i^*]}$  denotes to which score the threshold equals to.

Name	$\lambda_1$ (fp)	$\lambda_2$ (fn)	$t$ computed from	$i^*$
Prec@Rec	1	0	positive samples	$n^+ \alpha$
Rec@K	0	1	all samples	$K$
Pat&Mat	0	1	all samples	$n\alpha$
TopPush	0	1	negative samples	1
TopPushK	0	1	negative samples	$K$
Pat&Mat-NP	0	1	negative samples	$n\alpha$

### 3 DeepTopPush as a method for maximizing Accuracy at the top

Since the false-positives and false-negatives from (1) contain the discontinuous  $\mathbf{1}$  function, they are difficult to optimize. The standard approach is to replace them with a surrogate function  $l$  which is continuous non-decreasing (and usually convex with  $l(0) = 1$ ). This leads to

$$\begin{aligned} \underset{\mathbf{w}}{\text{minimize}} \quad & L(\mathbf{w}) := \lambda_1 \sum_{i \in I^-} l(z_i - t) + \lambda_2 \sum_{i \in I^+} l(t - z_i) \\ \text{subject to} \quad & z_i = f(\mathbf{w}; \mathbf{x}_i), \\ & t \text{ is a function of } \{z_i\}. \end{aligned} \tag{5}$$

We observe that the computation is nested. Having the input  $\mathbf{x}_i$  the classifier described by the weights  $\mathbf{w}$  computes the scores  $z_i$ , the threshold  $t$  and finally the loss function. Informally, we write this as  $\mathbf{w} \xrightarrow{\mathbf{x}_i} z_i \xrightarrow{} t \xrightarrow{y_i} L$ .

To apply the stochastic gradient descent we need to compute the (sub)gradients. Following the previous paragraph, we consider the network weights  $\mathbf{w}$  as the only optimization variable and denote the objective of (5) by  $L(\mathbf{w})$ . In all cases from Section 2, the threshold  $t$  always equals to one of the scores, let us denote it  $t = z_{j^*}$ . Then the chain rule implies (see details in Appendix C) that the gradient of the objective from (5) equals to

$$\begin{aligned} \nabla L(\mathbf{w}) = & \lambda_1 \sum_{i \in I^-} l'(z_i - t) (\nabla_{\mathbf{w}} f(\mathbf{w}; \mathbf{x}_i) - \nabla_{\mathbf{w}} f(\mathbf{w}; \mathbf{x}_{j^*})) \\ & + \lambda_2 \sum_{i \in I^+} l'(t - z_i) (\nabla_{\mathbf{w}} f(\mathbf{w}; \mathbf{x}_{j^*}) - \nabla_{\mathbf{w}} f(\mathbf{w}; \mathbf{x}_i)). \end{aligned} \tag{6}$$

Even though we could present methods for optimizing any criterion from Table 1, we propose our method *DeepTopPush*. It is based on *TopPush* [14], where the threshold equals to the highest score from negative samples and the objective contains only false-negatives (therefore  $\lambda_1 = 0$  and  $\lambda_2 = 1$ ). *TopPush* considers linear classifiers and solves (1) in its dual form. *DeepTopPush* extends *TopPush* to a nonlinear setting. We need to approximate the gradient (6) on a minibatch. Since

$\lambda_1 = 0$ , this gradient equals to

$$\nabla L(w) = \frac{1}{n^+} \sum_{i \in I^+} l'(t - z_i) (\nabla_w f(w; \mathbf{x}_{j^*}) - \nabla_w f(w; \mathbf{x}_i)). \quad (7)$$

We stress the dependence of  $t$  on  $\mathbf{z}$  by writing  $t(\mathbf{z})$  and similarly for  $j^*(\mathbf{z})$ . The standard technique is to replace the sum over all samples  $I$  with a sum over a minibatch  $I_{\min}$ . The situation for (6) is more complicated. As both the threshold  $t$  and the index  $j^*$  depend on all scores  $z_i$ , they need to be approximated on the minibatch as well. We denote these approximations by  $\hat{t}$  and  $\hat{j}$ , respectively. Then we replace the gradient from (7) by its “minibatch version”

$$\nabla L(w) \approx \nabla \hat{L} = \frac{1}{n_{\min}^+} \sum_{i \in I_{\min}^+} l'(\hat{t} - z_i) (\nabla_w f(w; \mathbf{x}_{\hat{j}}) - \nabla_w f(w; \mathbf{x}_i)). \quad (8)$$

While gradient descent schemes are fairly robust for approximated gradient [18], the threshold  $t$  has a large impact on the gradient. Since the threshold is computed from the scores  $z_i$ , we follow the idea from [1] and include the one negative sample from the previous minibatch with the largest score. As we will later in Figure 3, this significantly robustifies the threshold estimate.

We summarize *DeepTopPush* in Algorithm 3.1. Steps 3, 5, 7 and 8 follow the standard procedure of selecting the minibatch, approximating the gradient on the minibatch and updating the weights. The addition over the standard stochastic gradient descent lies in steps 4 and 6. In the former, we extend the minibatch by one sample. This delayed value from the previous minibatch allows for a more precise threshold approximation without the necessity to evaluate samples outside of the current minibatch. In the latter, we compute the threshold  $\hat{t}$  as the largest score corresponding to negative samples and find the index  $\hat{j}$  for which  $\hat{t} = z_{\hat{j}}$ . As we have mentioned earlier, we could use this procedure for any method from Table 1

---

**Algorithm 3.1** DeepTopPush as an efficient method for maximizing accuracy at the top.

---

- 1: Initialize weights  $w$ , threshold  $t$
- 2: **repeat**
- 3:   Select minibatch  $I_{\min}$
- 4:   Include one negative sample with highest value from the previous minibatch  $I_{\min}^{\text{enh}}$
- 5:   Computes scores  $z_i \leftarrow f(w; \mathbf{x}_i)$  for  $i \in I_{\min}^{\text{enh}}$
- 6:   Define  $\hat{t}$  as the largest score of negative samples and denote its index by  $\hat{j}$
- 7:   Approximate gradient  $\nabla L(w)$  by  $\nabla \hat{L}$  from (8)
- 8:   Make a gradient step
- 9: **until** stopping criterion is satisfied

---

## 4 Numerical experiments

In this section, we present numerical results for *DeepTopPush*. All codes were implemented in the Julia language [5] and are available online. First we provide technical details of the datasets and methods used. Then we show a comparison of methods on image recognition datasets, comparison with other papers, perform an ablation study and finally, we provide a real-world medical application of suggesting a small number of molecules for further research.

### 4.1 Dataset description

For numerical experiments, we consider the following image recognition datasets: MNIST [13], FashionMNIST [21], CIFAR10 [12], CIFAR100 [12] and SVHN2 [17]. All these datasets were converted to binary classification tasks by selecting one class as the positive class and the rest as the negative class. We also consider a 3A4 dataset [15] that contains records for nearly 50,000 molecules with their activity levels and 9491 descriptors. Descriptors are sparse and less than 4% are non-zero. All datasets are summarized in Table 2.

Table 2: Summary of the used datasets with the number of classes, which original labels  $y^+$  were selected as the positive class, sample size  $d$ , number of samples  $n$ , and the fraction of positive samples  $\frac{n^+}{n}$ .

	classes	$y^+$	$d$	Training		Testing	
				$n$	$\frac{n^+}{n}$	$n$	$\frac{n^+}{n}$
MNIST	10	0	$28 \times 28$	60 000	9.87%	10 000	9.80%
FashionMNIST	10	0	$28 \times 28$	60 000	10.00%	10 000	10.00%
CIFAR10	10	1	$32 \times 32 \times 3$	50 000	10.00%	10 000	10.00%
CIFAR100	100	1	$32 \times 32 \times 3$	50 000	5.00%	10 000	5.00%
SVHN2	10	1	$32 \times 32 \times 3$	73 257	18.92%	26 032	19.59%
SVHN2 extra	10	1	$32 \times 32 \times 3$	604 388	17.28%	26 032	19.59%
3A4	—	—	$9491 \times 1$	37 241	10.00%	12 338	10.40%

## 4.2 Performance criteria and Computational settings

All methods from Table 1 are compared to the *BaseLine* model. The *BaseLine* model uses the weighted cross-entropy as an objective

$$-\frac{1}{n^+} \sum_{i \in I^+} \log(\sigma(z_i)) - \frac{1}{n^-} \sum_{i \in I^-} \log(1 - \sigma(z_i)),$$

where  $z_i = f(\mathbf{w}; \mathbf{x}_i)$ . It does not consider any threshold and corresponds to the left-part only in Figure 1. We use the truncated quadratic loss  $l(z) = (\max\{0, 1 + z\})^2$  as the surrogate function.

During training, each dataset was divided into minibatches consisting of 32 samples. We implemented a condition that it needs to contain at least 5 positive samples. All algorithms were run for 100 epochs on a NVIDIA P100 GPU card. For the evaluation of numerical experiments, we use the standard performance metrics precision and recall. We also use  $\text{AUC@quantile}(\alpha)$  defined as the area under the  $P\tau$  curve where  $\tau \in [0, \alpha]$ . This curve is similar to the PR curve but it shows precision at the top  $\tau$ -quantile instead of recall. We describe the network architecture in Appendix D. During the convergence, we observed an interesting phenomenon which we show in Appendix F.

## 4.3 Numerical results: Method comparison

Besides *DeepTopPush* and the *BaseLine* method described in the previous subsection, we also consider two more representative methods from Table 1, namely *Prec@Rec* and *Patt&Mat*. We generalized Algorithm 3.1 and trained them in the same way as *DeepTopPush*. A fair comparison with prior arts requires the same running conditions including the same deep network. This, in turn, requires access to source codes. Unfortunately, we did not manage to find the source codes of any papers besides AP-Perf [9]. Since it is, as we will show later, computationally extremely expensive, we include it only in selected comparisons.

In Table 3 we show precision at different levels of recall averaged over all visual recognition datasets from Table 2 and over ten independent runs. The best result is depicted in green. All methods are better than the *BaseLine* method. This is not surprising for low levels of recall as the methods are designed to work well at these low levels. We believe that the reason why they work well at higher recall levels is that the sum in the objective is over only positive or negative samples. This evades the problem of imbalanced datasets. We show the PR curve with a focus on small recalls for CIFAR100 in Figure 2. Since *DeepTopPush* outperforms all other methods, we will show the following methods only for this method.

Table 3: The precision at a certain level of recall averaged across all visual datasets from Table 2 and ten runs. The best method in each column is highlighted in green.

	Precision at recall					
	0.05	0.1	0.2	0.4	0.6	0.8
BaseLine	96.11	95.37	91.38	89.87	84.61	75.92
Prec@Rec	97.36	94.73	93.34	90.92	85.82	76.44
Pat&Mat	96.99	96.04	94.28	90.06	85.63	76.36
DeepTopPush	99.07	98.46	97.05	93.44	89.56	79.50

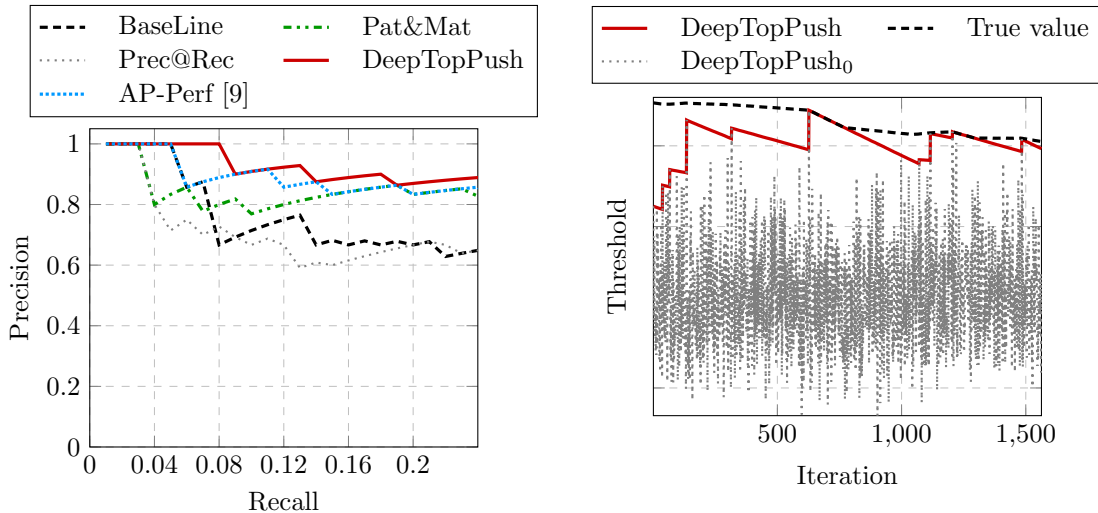


Figure 2: PR curve with focus on small recalls for the CIFAR100 dataset. Since all methods focus on working well on the top, they outperform the *BaseLine* approach.

Figure 3: Comparison of threshold estimates. While *DeepTopPush*<sub>0</sub> jumps chaotically, *DeepTopPush* provides a good and stable approximation of the true threshold.

#### 4.4 Numerical results: Ablation study

The ablation study determines which parts of an algorithm are necessary. The main ingredient for the computation of derivatives (6) is the chain rule, which considers the threshold as a function of network weights. Then the total derivative is a sum of a derivative of the objective with respect to the network weights and a derivative of the threshold with respect to network weights. Another approach [11] is to fix the threshold in each iteration and therefore ignore the second part from the previous sentence. In Appendix E we show that the second approach does not work in our setting and therefore, the chain rule is necessary.

The crucial part of our algorithm is the handling of the threshold. Besides the *DeepTopPush* method, it is also possible to ignore the delayed value from the previous iteration. We name this method *DeepTopPush*<sub>0</sub> because it corresponds to ignoring step 4 in Algorithm 3.1. *DeepTopPush* may propagate one sample over multiple iterations. We see this behaviour in Figure 3 which shows the second epoch of training at CIFAR100. While *DeepTopPush*<sub>0</sub> jumps randomly as the minibatch updates, *DeepTopPush* is a step function where each plateau corresponds to one fixed score index. Note that after six plateaus, the estimate reaches the true threshold, where it stays. This implies that *DeepTopPush* provides a good and stable estimate for the true threshold (which is computed on the whole dataset) while evaluating only one minibatch. In Table 4, we show AUC@quantile

averaged over ten runs. *DeepTopPush* outperforms the *DeepTopPush*<sub>0</sub> threshold update in most cases.

Table 4: Comparison of threshold computation averaged over ten runs. While *DeepTopPush*<sub>0</sub> computes the threshold only on one minibatch, *DeepTopPush* uses past score values to add robustness.

	AUC@quantile(0.1)		AUC@quantile(0.2)	
	DeepTopPush <sub>0</sub>	DeepTopPush	DeepTopPush <sub>0</sub>	DeepTopPush
MNIST	99.74	99.82	94.11	94.66
FashionMNIST	97.77	98.02	91.63	92.99
CIFAR10	97.67	97.69	92.98	92.95
CIFAR100	66.56	66.32	61.22	60.87
SVHN2	99.76	99.83	99.24	99.30
SVHN2 extra	99.84	99.81	99.45	99.47

Another comparison is presented in Figure 4 which shows a boxplot of 10 runs on CIFAR100. The thick horizontal line is the median, the diamond is the mean and the vertical lines represent the whiskers. The mean of *DeepTopPush* outperforms *DeepTopPush*<sub>0</sub> by approximately 1% while the best result is significantly better. Both *DeepTopPush* and *DeepTopPush*<sub>0</sub>, which are the accuracy at the top extension, give much better results than the *BaseLine* method.

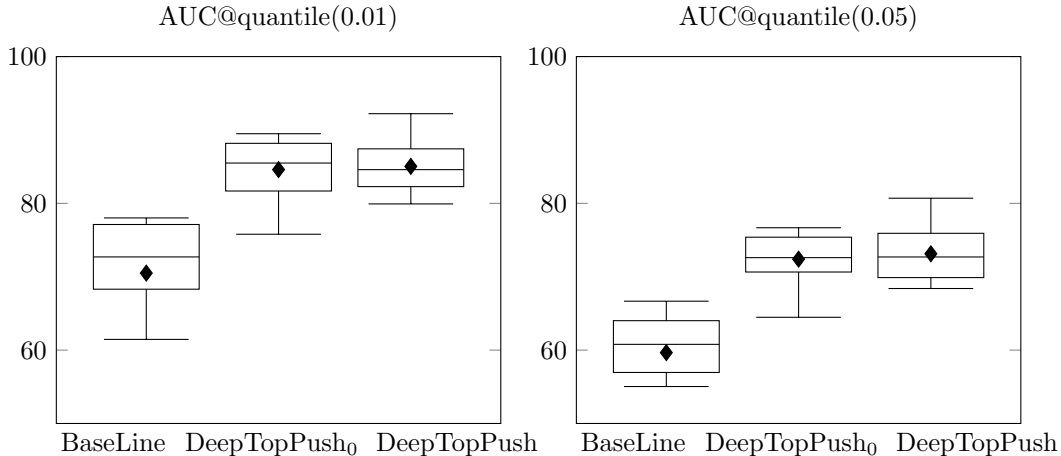


Figure 4: Comparison of the updates of threshold on 10 runs on the CIFAR100 dataset. The boxplots show the median (horizontal line), mean (diamond), interquartile range (box) and whiskers (vertical line).

#### 4.5 Numerical results: Comparison with prior art

A fair comparison with other methods requires the same running conditions including the same deep network. This, in turn, requires access to source codes. Unfortunately, we did not manage to find the source codes of any papers besides AP-Perf [9]. Table 5 shows that this algorithm is prohibitively slow. While our algorithm *DeepTopPush* shows an increase of computational times with respect to *BaseLine* of approximately 10-30%, the increase of AP-Perf reaches 4000%. It is possible to decrease the time for *DeepTopPush* at the expense of slightly larger memory requirements, we comment more on this in Appendix B. *DeepTopPush* is independent of the size of the minibatch. This is not true for AP-Perf whose time complexity grows exponentially as the minibatch size

increases. We provide further data for these claims in Appendix B. Therefore, *DeepTopPush* provides a significantly faster method than AP-Perf while not having worse performance as shown in Figure 2

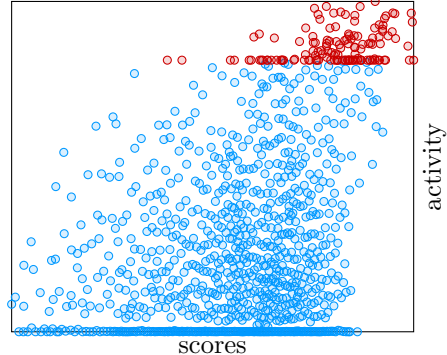
Table 5: Time increase over the *BaseLine* method per one epoch. While our method shows only a slight increase, the complexity of AP-Perf increases exponentially with minibatch size.

	Minibatch 32			Minibatch 128		
	BaseLine	DeepTopPush	APPerf [9]	BaseLine	DeepTopPush	APPerf [9]
MNIST	5.9s	+8%	+3976%	1.4s	+14%	+217000%
CIFAR100	5.1s	+25%	+3943%	3.0s	+30%	+ 72589%
SVHN2	7.6s	+25%	+3924%	4.4s	+30%	+ 73436%

## 4.6 Numerical results: Real-world application

In this final section, we show a real-world application of the accuracy at the top. The 3A4 dataset contains information about the activity of approximately 50,000 molecules, each with about 10,000 descriptors and 1 activity level. The activity level corresponds to the usefulness of the molecule for creating new drugs. Since medical scientists can focus on properly investigating only a small number of molecules, it is important to select a small number of molecules with high activity on the continuous testing set. This is precisely the accuracy at the top problem.

The activity level is continuous. We converted it into binary by considering a threshold on the activity on the training set. Since the input is rather large-dimensional and there is no spatial structure to use convolutional neural networks, we reduced the dimension into 100 by using the principal component analysis. Then we created a network with two hidden layers (described in Appendix D) and applied *DeepTopPush* to it. The test activity was evaluated at the continuous (and not discretized level). The figure on the right shows that high scores (output of the network) indeed correspond to high activity. Thus, even though the problem was “binarized” and its dimension reduced, our algorithm was able to select a small number of molecules with high activity levels. These molecules can be used for further manual (expensive) investigation.



## 5 Conclusions

In this paper, we proposed *DeepTopPush* an efficient method for solving the non-decomposable problem of accuracy at the top which focuses on the performance only above (or below) a threshold. We incorporated the threshold to create an end-to-end network and used the stochastic gradient descent to train it. We modified the threshold computation process so that the threshold estimate (computed on a minibatch) forms a good and stable estimate of the true threshold (computed on all samples). The time increase over the standard method with no threshold was relatively small. We demonstrated the usefulness of our method both on visual recognition datasets and on a real-world application where the goal is to suggest a few potential molecules for further study.

## Broader Impact

The paper presents a general method applicable to any field where only a small number of samples can be manually processed. We demonstrated its usefulness on the 3A4 dataset where we successfully

suggested molecules with large activity. Our codes are online and full documentation is provided. Users with minimal knowledge of machine learning may therefore easily use them.

## References

- [1] L. Adam and M. Branda. Machine learning approach to chance-constrained problems: An algorithm based on the stochastic gradient descent. *arXiv preprint arXiv:1905.10986*, 2019.
- [2] L. Adam, V. Mácha, V. Šmíd, and T. Pevný. General framework for binary classification on top samples. *arXiv preprint arXiv:2002.10923*, 2019.
- [3] S. Agarwal. The infinite push: A new support vector ranking algorithm that directly optimizes accuracy at the absolute top of the list. In *Proceedings of the 2011 SIAM International Conference on Data Mining*, pages 839–850. SIAM, 2011.
- [4] Z. Batmaz, A. Yurekli, A. Bilge, and C. Kaleli. A review on deep learning for recommender systems: challenges and remedies. *Artificial Intelligence Review*, 52(1):1–37, 2019.
- [5] J. Bezanson, A. Edelman, S. Karpinski, and V. B. Shah. Julia: A fresh approach to numerical computing. *SIAM review*, 59(1):65–98, 2017.
- [6] S. Boyd, C. Cortes, M. Mohri, and A. Radovanovic. Accuracy at the top. In *Advances in neural information processing systems*, pages 953–961, 2012.
- [7] E. Eban, M. Schain, A. Mackey, A. Gordon, R. A. Saurous, and G. Elidan. Scalable learning of non-decomposable objectives. *arXiv preprint arXiv:1608.04802*, 2016.
- [8] M. Engilberge, L. Chevallier, P. Pérez, and M. Cord. Sodeep: a sorting deep net to learn ranking loss surrogates. In *Proceedings of the IEEE Conference on Computer Vision and Pattern Recognition*, pages 10792–10801, 2019.
- [9] R. Fathony and J. Z. Kolter. Ap-perf: Incorporating generic performance metrics in differentiable learning. In *Proceedings of the 23rd International Conference on Artificial Intelligence and Statistics (AISTATS)*, 2020.
- [10] Y. Freund, R. Iyer, R. E. Schapire, and Y. Singer. An efficient boosting algorithm for combining preferences. *The Journal of machine learning research*, 4:933–969, 2003.
- [11] M. Grill and T. Pevný. Learning combination of anomaly detectors for security domain. *Computer Networks*, 107:55–63, 2016.
- [12] A. Krizhevsky, G. Hinton, et al. Learning multiple layers of features from tiny images. 2009.
- [13] Y. LeCun, L. Bottou, Y. Bengio, and P. Haffner. Gradient-based learning applied to document recognition. *Proceedings of the IEEE*, 86(11):2278–2324, 1998.
- [14] N. Li, R. Jin, and Z.-H. Zhou. Top rank optimization in linear time. In *Advances in neural information processing systems*, NIPS’14, pages 1502–1510, Cambridge, MA, USA, 2014. MIT Press.
- [15] J. Ma, R. P. Sheridan, A. Liaw, G. E. Dahl, and V. Svetnik. Deep neural nets as a method for quantitative structure–activity relationships. *Journal of chemical information and modeling*, 55(2):263–274, 2015.
- [16] V. Mácha, L. Adam, and V. Šmíd. Nonlinear classifiers for ranking problems based on kernelized SVM. *arXiv preprint arXiv:2002.11436*, 2020.
- [17] Y. Netzer, T. Wang, A. Coates, A. Bissacco, B. Wu, and A. Y. Ng. Reading digits in natural images with unsupervised feature learning. 2011.

- [18] J. Nocedal and S. Wright. *Numerical optimization*. Springer Science & Business Media, 2006.
- [19] C. Rudin. The p-norm push: A simple convex ranking algorithm that concentrates at the top of the list. *Journal of Machine Learning Research*, 10(Oct):2233–2271, 2009.
- [20] T. Werner. A review on ranking problems in statistical learning. *arXiv preprint arXiv:1909.02998*, 2019.
- [21] H. Xiao, K. Rasul, and R. Vollgraf. Fashion-mnist: a novel image dataset for benchmarking machine learning algorithms, 2017.

## A Additional material

In this section, we provide the definition of precision and recall and comment more on methods from Table 1. Precision and recall are defined by

$$\begin{aligned} \text{Precision} &= \frac{\text{tp}(\mathbf{z}, t)}{\text{tp}(\mathbf{z}, t) + \text{fp}(\mathbf{z}, t)} = \frac{\sum_{i \in I^+} \mathbf{1}_{z_i \geq t}}{\sum_{i \in I} \mathbf{1}_{z_i \geq t}}, \\ \text{Recall} &= \frac{\text{tp}(\mathbf{z}, t)}{\text{tp}(\mathbf{z}, t) + \text{fn}(\mathbf{z}, t)} = \frac{\sum_{i \in I^+} \mathbf{1}_{z_i \geq t}}{n^+}. \end{aligned} \quad (9)$$

Problems of type (1) appeared in multiple instances in the literature, we mention the following cases.

**Rec@K and Pat&Mat** Rec@K maximizes recall under the condition that the threshold equals to the top  $K$ -component of  $\mathbf{z}$ . Similarly, Pat@Mat from [2] maximizes recall under that condition that the threshold equals to the  $n\alpha$ -top component of  $\mathbf{z}$ . Since maximizing recall is equivalent to minimizing false-negatives due to (9), we arrive at

$$\begin{aligned} &\underset{w}{\text{minimize}} \quad \text{fn}(\mathbf{z}, t) \\ &\text{subject to} \quad z_i = f(\mathbf{w}, \mathbf{x}_i), \\ &\quad t = z_{[i^*]}, \quad i^* = K \text{ (Rec@K); or } i^* = \alpha n \text{ (Pat@Mat)}. \end{aligned} \quad (10)$$

**TopPush, TopPushK, Pat@Mat-NP** TopPush [14], TopPushK and Pat&Mat-NP [2] have the same structure as (10) with the difference that the quantile is computed only from negative samples. This leads to

$$\begin{aligned} &\underset{w}{\text{minimize}} \quad \text{fn}(\mathbf{z}, t) \\ &\text{subject to} \quad z_i = f(\mathbf{w}, \mathbf{x}_i), \\ &\quad t = z_{[i^*]}^-, \quad i^* = 1 \text{ (TopPush); } i^* = K \text{ (TopPushK); } i^* = n\tau \text{ (Pat@Mat-NP)}. \end{aligned} \quad (11)$$

All problems from this section fall into the setting (1). We provide a summary in Table 1. We would like to mention two observations. First, no surrogates were used so far. Second, threshold  $t$  always equals to one of the scores which will be used in the next section when computing derivatives.

## B Computational time

A crucial part of the gradient from (8) takes form

$$\sum_{i \in I_{\min}^+} l'(\hat{t} - z_i) \nabla_w f(\mathbf{w}; \mathbf{x}_i).$$

There are two ways to compute this sum. The first one is to compute  $\nabla_w f(\mathbf{w}; \mathbf{x}_i)$  for all indices  $i$  from the minibatch. Since the gradient computation is a backward pass, a forward pass, which computes  $z_i$ , will be performed at the same time. However, this has larger memory requirements, as  $\nabla_w f(\mathbf{w}; \mathbf{x}_i)$  need to be stored in the memory and only then the sum may be computed. The second option is to perform the scores  $z_i$  first and then, embed the computation of the sum into the `map` command. This results in much lower memory requirements. However, the scores will be computed two times as they will be recomputed in the computation of  $\nabla_w f(\mathbf{w}; \mathbf{x}_i)$ . In the codes, we implemented the second method. Therefore, it should be possible to reduce the computational times in Table 5 but the price would be higher memory requirements.

In Table 6 we show that the complexity of AP-Perf [9] increases exponentially with the minibatch size. This is in sharp contrast with Table 5 which shows that the required time per epoch for our approach decreases as the minibatch size increases.

Table 6: Computation time in seconds for AP-Perf [9] per epoch. The time grows exponentially in the minibatch size.

	Minibatch size		
	32	64	128
FashionMNIST	240	577	3039
CIFAR100	206	497	2181
SVHN2	306	663	3236

## C Computation of derivatives

In this short section, we show the formal computation of derivatives in (6). Since the threshold  $t$  depends on the weights  $\mathbf{w}$ , from the chain rule we get

$$\nabla_w t = \sum_{i \in I} \nabla_{z_i} t \nabla_w z_i.$$

Even though it is possible to continue with this general dependence, we present only the simpler case where we have  $t = z_{j^*}$  for some  $j^*$ . Note that this covers all examples from Section 2. Then the previous derivative reduces to

$$\nabla_w t = \nabla_{z_{j^*}} t \nabla_w z_{j^*} = \nabla_w z_{j^*}. \quad (12)$$

Using the chain rule again, we arrive at

$$\begin{aligned} \nabla_w l(t - z_i) &= l'(t - z_i) (\nabla_w t - \nabla_w z_i) = l'(t - z_i) (\nabla_w z_{j^*} - \nabla_w z_i) \\ &= l'(t - z_i) (\nabla_w f(\mathbf{w}; \mathbf{x}_{j^*}) - \nabla_w f(\mathbf{w}; \mathbf{x}_i)), \end{aligned}$$

where in the second equality we used (12) and in the last one the relation  $z_i = f(\mathbf{w}; \mathbf{x}_i)$ . Using the structure of the objective of (5), we immediately arrive at (6).

## D Used network architecture

For 3A4 we preprocessed the input with 9491 into a 100-dimensional input by PCA. Then we used two dense layers of size  $100 \times 50$  and  $50 \times 25$  with batch-normalization after these layers. The last layer was dense.

For MNIST and FashionMNIST we used a network alternating two hidden convolutional layers with two max-pooling layers finished with a dense layer. The convolutional layers used kernels  $5 \times 5$  and had 20 and 50 channels, respectively. For the remaining datasets, we increased the number of

hidden and max-pooling layers from two to three. The convolutional layers used kernels  $3 \times 3$  and had 64, 128 and 128 channels, respectively. A more detailed description can be found in our codes online.

## E Failure of a naive approach

In the ablation study we mentioned that it is important to consider the chain rule for the computation of derivatives. The naive approach fixes the threshold in every iteration and ignores that it depends on the weights of the network. This corresponds to replacing the gradient (7) by

$$\nabla L(w) = -\frac{1}{n^+} \sum_{i \in I^+} l'(t(\mathbf{z}) - z_i) \nabla_w f(\mathbf{w}; \mathbf{x}_i). \quad (13)$$

Now consider the dataset depicted in Figure 5 and the linear classifier  $f(\mathbf{w}; \mathbf{x}) = w_1 x_1 + w_2 x_2$ .

Assume that the current weights are  $\mathbf{w} = (w, 0)$  with  $w > 0$ . Since the goal is to rank positives above negative, this generates an (almost) perfect separation. Since  $t = 3w$ , with the hinge loss, then the first component of the gradient (13) takes form

$$\nabla L(w) = -\frac{1}{n^+} \sum_{i \in I^+} x_{i,1} \approx -\frac{1}{2}.$$

This means that for an arbitrarily small stepsize, the classifier diverges to infinity. The problem is that the gradient (13) tries to push positives above negatives but ignores the fact that when the scores of the former are increased, the threshold increases as well.

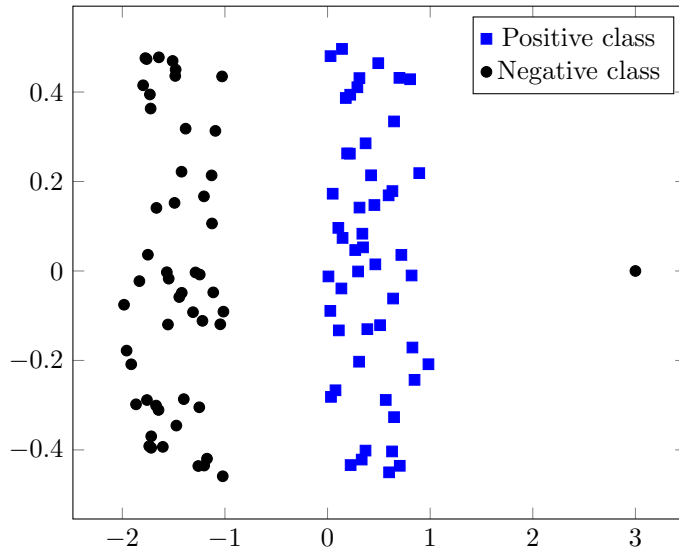


Figure 5: A simple example where a naive approach fails.

## F Stability of the objective function

In Figure 6 we show an interesting phenomenon of the accuracy at the top. It shows the objective value for 10 runs on the CIFAR100 dataset both on the training and testing set. The objective value decreases to almost zero on the training set. Even though this may suggest some overfitting, it also indicates that our method and the threshold update converge. However, on the testing set, the figure shows a different behaviour and the objective value even increases for all runs.

The reason for this is that even though standard deep networks are stable when a new sample is added, this does not hold for the accuracy at the top. Since the threshold equals the highest score corresponding to negative samples, a single new sample may shift the threshold significantly. This, in turn, changes the objective significantly even though the separation quality barely changed. Therefore, the validation set should never consider the value of the objective function but it needs to consider the accuracy which is more stable.

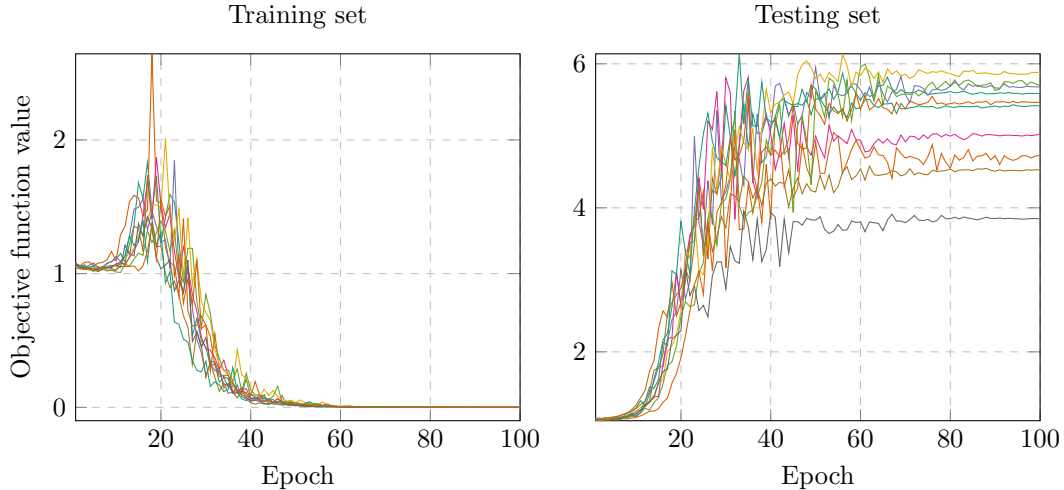


Figure 6: Multiple runs on the CIFAR100 dataset show the different behaviour of the loss function on the training and testing function. As we show in Figure 7, this is not unexpected and the classifier works normally.

The previous paragraph suggests that even though the objective function increases on the testing set, the classifier works. This is confirmed in Figure 7 where we show AUC@quantile. We see that it increases both on the training and testing sets. This, together with the previous paragraph, implies that the discrepancy from Figure 6 is actually not harmful.

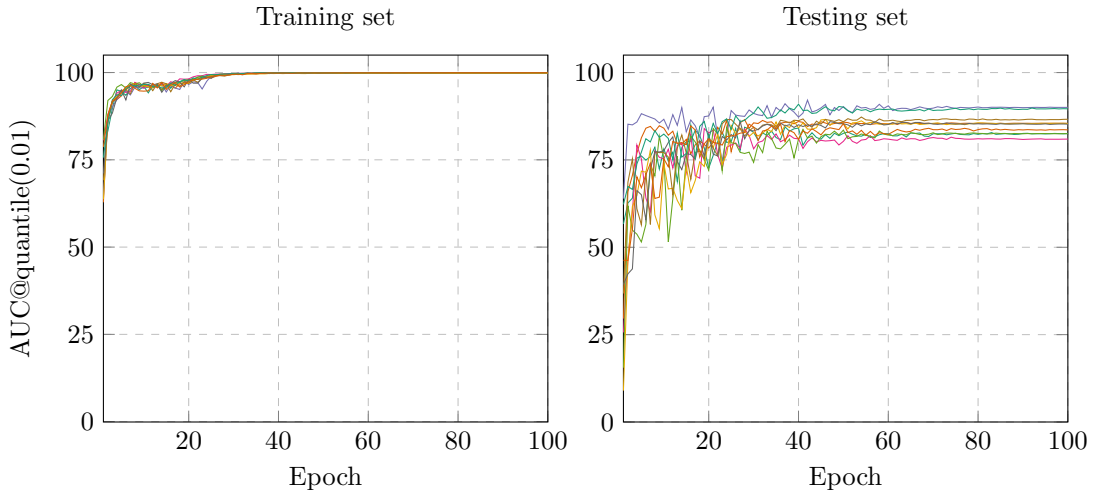


Figure 7: Multiple runs on the CIFAR100 dataset show that the correct performance measure increases both on the training and testing set.